Vacuum 130 (2016) 109–112

Contents lists available at ScienceDirect

Vacuum

journal homepage: www.elsevier.com/locate/vacuum

Short communication

Resistive switching memory based on organic/inorganic hybrid perovskite materials

Yang Liu [a], Fushan Li [a, *], Zhixin Chen [a], Tailiang Guo [a], Chaoxing Wu [b], Tae Whan Kim [b]

[a] Institute of Optoelectronic Technology, Fuzhou University, Fuzhou 350002, People's Republic of China
[b] Department of Department of Electronics and Computer Engineering, Hanyang University, Seoul 133-791, Republic of Korea

ARTICLE INFO

Article history:
Received 26 February 2016
Received in revised form
7 May 2016
Accepted 9 May 2016
Available online 10 May 2016

Keywords:
Perovskite
Memory
Resistive switching

ABSTRACT

In this work, a resistance switching memory based on organic/inorganic hybrid perovskites (OIHPs) was fabricated. The $CH_3NH_3PbI_3$ perovskite was grown on polymethyl methacrylate (PMMA) as the resistance switching layer by using a two-step spin-coating procedure. The conduction mechanisms of indium-tin-oxide (ITO)/PMMA/$CH_3NH_3PbI_3$/PMMA/Ag device were investigated in terms of current–voltage characteristics. The memory device is reprogrammable and the ON/OFF ratio reaches as high as 10^3. Endurance cycle of the as-fabricated memory device was also carried out. The results indicate the promising electronic application of OIHPs in resistance switching memories.

1. Introduction

With the demands for high density and good performance memory in portable electronic devices continuously increasing, the resistive random access memories (RRAMs) have recently attracted quite a lot attentions due to a variety of advantages including simple structure, high memory density, low fabrication cost and low power consumption [1–4]. In order to improve the performance of RRAMs, storage media have been expanded to nanoparticles [5], binary metal oxides [6], organic material [7], graphene [8] and even perovskite. Resistance switching memory with perovskite oxides has been proved to have a good performance in previous reports [1,9,10], but few works focus on organic/inorganic hybrid perovskites (OIHPs) based resistance switching memory. In comparison with traditional semiconducting materials, OIHPs combine the superior properties of organic materials and inorganic materials such as high charge-carrier mobility, balanced electron/hole mobility, small exciton binding energy, low cost, flexibility, easy processing, facile tuning of optical and electrical properties [11–14]. Because of these properties, OIHPs have been becoming a kind of promising material in photoactive layers of solar cells and light emitting diode, even though the inferior stability to moist air and water vapor, and the usage of lead as a key component [15–20]. The OIHPs based RRAM devices could be fabricated in flexibility and in a solution-processed way, compared with mainstream resistive RRAMs based on metal oxides corresponding to high temperature process and breakable hard structures. Yoo et al. have fabricated the Au/$CH_3NH_3PbCl_xI_{3-x}$/FTO resistive switching memory devices with ON/OFF current ratio less than 10^1 [21].

In this work, we fabricated the resistance switching memory devices with metal–insulator–metal (MIM) structure based on OIHPs. Poly(methyl methacrylate) (PMMA) layer was used as charge blocking layers for its easy coating way of spin-coating, smooth surface and thermal stability [22]. $CH_3NH_3PbI_3$was used as charge trapping layer to form charge traps. Memory devices show memory effect and excellent ratio of over 10^3 which is much better than the previous result [21]. In addition, the memory performances were investigated systematically and the memory mechanisms were discussed on the basis of the I–V results.

2. Experimental details

A metal-insulator-metal (MIM) sample with a structure of indium-tin-oxide (ITO)/PMMA/$CH_3NH_3PbI_3$/PMMA/Ag device was fabricated, as shown in Fig. 1. Two kinds of PMMA solutions were prepared by dissolving 20 mg and 50 mg PMMA powder in 1 ml chlorobenzene, respectively, and then continuously stirred for 5 h. ITO-coated glass substrates were cleaned by ultrasonication successively in deionized (DI) water, acetone, isopropanol and DI water. Then, nitrogen stream was used to dry the substrate, followed

* Corresponding author.
E-mail address: fushanli@hotmail.com (F. Li).

http://dx.doi.org/10.1016/j.vacuum.2016.05.010
0042-207X/

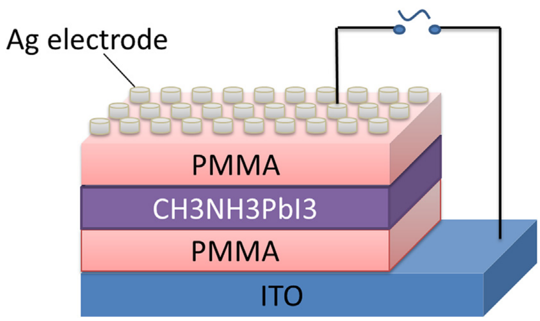

Fig. 1. Schematic architecture of the as-fabricated memory device.

by 10 min oxygen plasma treatment. The fabrication of the memory device began with the spin coating of PMMA (20 mg/ml) on top of the cleaned ITO substrate. After this, the film was heated at 120 °C for 30 min $CH_3NH_3PbI_3$was formed by using a two-step spin coating procedure. PbI_2 solution was prepared by dissolving 462 mg PbI_2 (99%, Aldrich) in 1 ml *N*,*N*-dimethylformamide (DMF) from Sigma-Aldrich under stirring at 70 °C for 2 h PbI_2 solution was spin-coated on the PMMA film at 3000 rpm for 5 s (without loading time). After spinning, the film was dried at 40 °C for 7 min and then 100 °C for 1 min, and then cooled to room temperature. 250 µl of 8 mg/ml CH_3NH_3I solution in 2-propanol was loaded on the PbI_2-coated substrate for 20 s (loading time), which was spun at 4000 rpm for 20 s and dried at 100 °C for 5 min. PMMA solution (50 mg/ml) was chosen to form another layer of PMMA by spin coating at 3000 rpm for 40 s. Finally, 64 circular Ag electrodes with a diameter of 0.5 mm were formed by thermal evaporation using a shadow mask. The current–voltage (I–V) characteristics of the device were measured with a semiconductor characterization system (Keithly4200-SCS). Bias voltages were applied to the top metal electrode with respect to ITO for all measurements.

3. Results and discussion

The surface morphologies of $CH_3NH_3PbI_3$ on PMMA layer have been characterized by atomic force microscopy (AFM) and the result are shown in Fig. 2. The results indicated that the high quality $CH_3NH_3PbI_3$ layer was obtained in our experiments. The typical I–V characteristics (measured from −4 to 3 V and from 3 to −4 V) of the ITO/PMMA/$CH_3NH_3PbI_3$/PMMA/Ag device are shown in Fig. 3. The

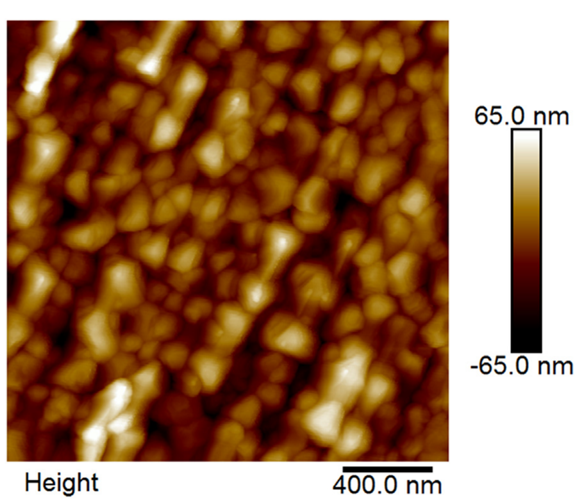

Fig. 2. AFM image of $CH_3NH_3PbI_3$ on PMMA layer.

hysteresis behaviors of the devices are clearly shown, implying that the ITO/PMMA/$CH_3NH_3PbI_3$/PMMA/Ag device can work as a resistive switching memory.

The ITO/PMMA/$CH_3NH_3PbI_3$/PMMA/Ag device showed OFF state (low-current state) during the sweep from −4 to 0 V. A dramatic increase in current at about 1.2 V (V_{ON}) indicated the transition of the device from the OFF state (low-current state) to ON state (high-current state) when voltage was swept from 0 to 3 V. The ITO/PMMA/$CH_3NH_3PbI_3$/PMMA/Ag device was maintained at ON state (high-current state) when voltage was reversed from 3 to 0 V. Finally, the ITO/PMMA/$CH_3NH_3PbI_3$/PMMA/Ag device shifted dramatically to OFF state at −3.3 V when voltage was continuously swept from0to −4 V. For the ITO/PMMA/$CH_3NH_3PbI_3$/PMMA/Ag device, the ratio of the ON/OFF current (I_{on}/I_{off}) achieved between the two states at a voltage of 0.45 V reached about 10^3. The I–V curve shows the ITO/PMMA/$CH_3NH_3PbI_3$/PMMA/Ag device has a quite low V_{ON} and high I_{on}/I_{off}.

Several possible conduction mechanisms could be used to explain the hysteresis of the resistive random access memories, such as, the Simmons and Verderber (SV) model [23], thermionic emission (TE) conduction mechanism [24,25], trapped-charge limited-current (TCLC) [26,27], Ohmic current model [26], and space-charge-limited current (SCLC) mechanism [28–30].

In the I–V curve, the SV model fails to explain it since the I–V curve is not N-shaped [23]. In order to explain the possible transport mechanisms, the ln(*I*)-ln(*V*) curves of the device are shown in Fig. 3 and were divided into three regions①, ② and ③. In region ①, ln(*I*) is proportional to $V^{1/2}$, as shown in the inset of Fig. 3(b), indicating that the TE conduction mechanism could fit well with the data at low voltage from 0 to 0.75 V. This phenomenon shows that there are thermally generated free carriers at the interface between the electrode and the organic layers.

In region ② (from 0.8 to 1.2 V), the slope of the fitting line was about 2.3 (close to 2), indicating that I is proportional to V^2, which is well fitted with SCLC mechanism. It is well known that the SCLC mechanism is closely related to the charge-carrier trapping or detrapping by defects, as well as dielectric parameters of the switching layer. When $CH_3NH_3PbI_3$ was fabricated on PMMA by using two-step spin coating procedure, traps were formed. A lot of reports about trap states of $CH_3NH_3PbI_3$ have been published [31–33]. The trap states of $CH_3NH_3PbI_3$ would affect the properties of solar cells, but indicate the promising electronic application of perovskites in resistive random access memories. A possible explanation of the conduction mechanism in our device could be the defects inside the $CH_3NH_3PbI_3$. To prove our hypothesis, ITO/PMMA/Ag and ITO/$CH_3NH_3PbI_3$/Ag devices were fabricated and the I–V curve was shown in Fig. 3(c) and (d), respectively. The ITO/PMMA/Ag device did not exhibit any memory effect during the forward and reverse biased sweeps. The ITO/$CH_3NH_3PbI_3$/Ag devices exhibit a quite small memory effect with the ON/OFF current ratio less than 10, which is consistent with the result of Yoo et al. However the defects inside the $CH_3NH_3PbI_3$ couldn't account for the ON/OFF current ratio of about 10^3. The main reason could be the charge trapping at the interface between $CH_3NH_3PbI_3$ and the PMMA layer. When bias is applied to the electrodes, injected electrons will be trapped by interface traps until they were occupied and the trapped electrons will form a reversed electric field at the interface. In this model, trapped electrons act as space charges to limit the current as reported by J Chen et al. [34].

Finally, the slope is close to 1 (n = 1.2) in region ③ (after the device switches to high-current state), indicating that it is fitted well with Ohmic current model. This could be understood that all the traps are completely filled up in the former periods and then much less negative carriers from the cathode are trapped. As a result, the device is less affected by the scanning direction of the